

## Original Article

# Epithelioid hemangioendothelioma: evaluation by $^{18}\text{F}$ -FDG PET/CT

Livia Maria Frota Lima, Annie T Packard, Stephen M Broski

Department of Radiology, Mayo Clinic, Rochester, MN, USA

Received February 5, 2021; Accepted March 31, 2021; Epub April 15, 2021; Published April 30, 2021

**Abstract:** Purpose: The purpose of this study was to evaluate the imaging characteristics of epithelioid hemangioendothelioma (EHE) on staging  $^{18}\text{F}$ -FDG PET/CT. Materials and methods: An IRB-approved retrospective review was conducted for patients with biopsy-proven EHE who underwent FDG PET/CT at our institution between 2005 and 2019. Patients with a history of surgery, chemotherapy, or radiotherapy prior to PET/CT were excluded. PET/CT exams were analyzed, noting metabolic activity, distribution of involvement, and CT morphologic features. PET/CT findings were correlated with comparative CT and MRI performed within three months. Results: There were 35 patients [21 females, 14 males; average age  $55.1 \pm 16.9$  years (range 15-82 years)]. 18/35 patients (52%) had more than one organ affected on PET/CT. The most common sites were liver [21/35 (60%)], lung [(19/35 (54%))], bone [5/35 (14%)], lymph nodes [4/35 (11%)], and vasculature [4/35 (11%)]. Most patients [30/35, (86%)] presented with multiple lesions. The average largest lesion dimension was  $4.0 \pm 3.6$  cm (range 0.6-15.0 cm). The average SUVmax of the most metabolically active lesion at any site was  $5.3 \pm 3.3$  (range 1.2-17.1), and for bone was  $7.9 \pm 5.4$  (range 3.5-17.1), liver was  $5.1 \pm 2.1$  (range 2.6-10.5), and lung was  $3.0 \pm 1.9$  (range 1.2-8.5). Of patients with pulmonary lesions, 9/19 (47%) showed calcification, and 4/19 (21%) had nodules that were either non FDG-avid or too small for accurate SUV assessment. Of patients with hepatic lesions, 11/21 (52%) demonstrated capsular retraction, and 12/21 (57%) were found to have additional hepatic lesions on contrast-enhanced CT or MRI that were occult on PET/CT. Conclusion: EHE demonstrates variable, but most commonly moderate FDG activity on PET/CT. The most common sites of disease are the liver, lungs, and bones, and most patients present with multiple lesions and more than one organ involved. Given the intrinsic metabolic activity and multi-organ involvement, FDG PET/CT represents an attractive modality for EHE evaluation. However, it may be best used in combination with CT or MRI given that EHE pulmonary or hepatic lesions may be missed by PET/CT.

**Keywords:** Epithelioid hemangioendothelioma, PET/CT, EHE, staging

## Introduction

Epithelioid hemangioendothelioma (EHE) is a rare vascular malignancy with an epithelioid and histiocytoid appearance, originating from vascular endothelial or pre-endothelial cells. It was described for the first time in 1975 by Dail and Liebow as pulmonary EHE (P-EHE) [1]. Initially, it was believed to be an aggressive form of bronchoalveolar cell carcinoma, invading adjacent blood vessels and small airways. The term epithelioid hemangioendothelioma was introduced in 1982 by Weiss and Enzinger who evaluated 41 cases of solid tumors, which had a vascular origin with intermediate features between hemangioma and angiosarcoma [2, 3]. In the 2013 World Health Organization

classification of sarcomas, EHE was categorized as a malignant tumor distinct from other vascular tumors [4]. EHE shows low to intermediate grade malignant features, and its clinical behavior is more indolent than angiosarcoma.

EHE is rare, representing less than 1% of all the vascular tumors. Most commonly it affects the lungs, liver, or bones, although it can occur primarily in almost any site, including the scalp, nasal cavity, cervix, and even the tongue [5]. EHE is often incidentally diagnosed, and up to 50-76% of patients are asymptomatic. Among patients with symptomatic disease, pain is the most commonly reported symptom. Other presenting symptoms depend on disease site; for example, hepatic EHE may cause constitutional

symptoms, nausea and jaundice, and pulmonary involvement may result in dyspnea, cough, and hemoptysis. Because of the variable presentation and rarity, EHE may be misdiagnosed, leading to delayed treatment. There are no specific laboratory tests for EHE [6]. Treatment options for EHE are individualized for each patient based on the number of lesions, tumor growth, involved organs and patient symptoms. For single lesions, surgical resection is the optimal treatment, and hepatic transplantation may be used for localized liver disease. Radiotherapy is suitable for patients with lesions involving the bones [7, 8], while chemotherapy may have utility in patients with advanced disease or with lesions not amenable to surgery or radiation therapy [9, 10]. Limited response rates have been demonstrated with targeted therapies, including anti-angiogenic agents [11-13]. In asymptomatic patients with diffuse lesions, watchful waiting is an acceptable option and spontaneous regression has been reported [14].

Imaging is important in EHE to determine lesion resectability, stage, assess response to therapy, and evaluate for local recurrence following primary treatment. To date, most imaging studies have focused on the CT and MRI appearances of hepatic EHE [15, 16], and CT appearance of pulmonary EHE [17, 18]. In comparison, there is relatively limited data regarding the  $^{18}\text{F}$ -fluorodeoxyglucose positron emission tomography/computed tomography ( $^{18}\text{F}$ -FDG PET/CT) features of EHE, which consists primarily of case reports [19, 20] and small series [21, 22]. Therefore, the purpose of this study was to evaluate the imaging features of EHE on staging FDG PET/CT in a large cohort of pathologically proven EHE patients.

## Materials and methods

This Health Insurance Portability and Accountability Act-compliant retrospective study was approved by our institutional review board. The requirement for informed consent was waived for this study. Pathology and imaging databases were searched for cases of pathologically-proven EHE from 01/01/2005 to 12/31/2019. Pathological diagnosis was established by biopsy and/or surgical resection. Only staging exams were included; patients with a history of surgery, chemotherapy or radiotherapy prior to PET/CT were excluded.

The electronic medical record was searched, and various data were collected and analyzed, including patient age, gender, biopsy results and treatment history. The imaging database was cross-referenced for any correlative CT and/or magnetic resonance imaging (MRI) performed within three months of PET/CT. All available follow-up chest CTs were analyzed to determine growth rate and evolution of pulmonary lesions.

PET/CTs (Discovery RX, 690 710, or MI; GE Healthcare, Waukesha, WI; USA) were performed according to the standard clinical protocol. PET/CT machines were regularly cross-calibrated against a dose-calibrated phantom standard to ensure consistency and reproducibility and activity recovery coefficients monitored for stability per institutional quality assurance protocol and American College of Radiology (ACR) accreditation guidelines. Parameters including height, weight and serum blood glucose were recorded for all patients. All patients had a blood glucose level of less than 200 mg/dl, and were administered 10-15 mCi of  $^{18}\text{F}$ -FDG, with an incubation period of 60-70 minutes. The amount of injected radioactivity was routinely measured by means of quantifying the radioactivity within the syringe before and after injection or with an automated injection system (Medrad® Intego PET infusion system, Bayer Healthcare, Whippany, NJ, USA). Patients were imaged covering at least from orbits to mid-thighs with 2D or 3D ordered subset expectation maximization, two iterations, Gaussian post-filter smoothing with a full width at half maximum of 7 mm,  $128 \times 128$  matrix, 3-5 minutes per bed position depending on body mass index. Low-dose helical CT images were obtained for attenuation correction and anatomic localization.

MIM software (MIM Software Inc., Cleveland, Ohio; United States) was used for PET/CT analysis and Visage software (Pro Medicus, Richmond, Victoria; Australia) for CT and MRI analysis. PET/CT imaging characteristics analyzed included maximal standardized uptake value (SUVmax), distribution of involvement, number of affected organs, number of lesions in each organ, maximal dimension, and morphologic CT features such as the presence and characterization of calcification in pulmonary lesions and capsular retraction associated with hepatic lesions. Lesions were considered posi-

**Table 1.** Patient demographics and disease sites

Age (years)	55.1±16.9
Sex	
Male	14/35 (40%)
Female	21/35 (60%)
Affected sites	
Liver	21/35 (60%)
Lung	19/35 (54%)
Bone	5/35 (14%)
Lymph nodes	4/35 (11%)
Supraclavicular region	4/35 (11%)

tive if metabolic activity exceeded that of the liver. Pulmonary nodules with follow-up images were analyzed and volume doubling time (VDT) was calculated using the following formula:  $VDT \text{ (days)} = \ln(2) \times \Delta t / \ln(V2/V1)$  where  $\Delta t$  is the time (days) between CT scans;  $V1$  and  $V2$  are the initial volume and following volume respectively. Volume was estimated by manually calculating the cube of the maximum dimension of the nodule and afterwards divided by 2 to avoid overestimation of the volume [23].

Statistical analysis was performed using JMP software on a Mac (JMP Pro, version 11.2.1, SAS Institute Inc.). Continuous variables are expressed as mean  $\pm$  SD. Categorical variables are presented with absolute and relative frequencies. *P*-values for between-group comparisons of continuous data were calculated from Kruskal-Wallis one-way analysis of variance. Statistical significance was established for *p* values of less than 0.05.

## Results

There were 35 patients (21 females, 14 males) with pathologically-proven EHE and staging PET/CT prior to treatment included. The average age at diagnosis was 55.1±16.9 years (range 15-82). 18/35 patients (52%) had more than one organ affected on PET/CT. The most common sites were liver [21/35 (60%)], lung [19/35 (54%)], bone [5/35 (14%)], lymph nodes [4/35 (11%)] and the supraclavicular vasculature [4/35 (11%)]. Less common locations included mediastinum [2/35 (6%)], retroperitoneum [1/35 (3%)], paracolic soft tissues [1/35 (3%)] and gluteal musculature [1/35 (3%)].

3/35 (9%) had both lung and liver involvement and only 1/35 (3%) had isolated bone involvement. Most patients [30/35 (86%)] presented with multiple lesions, including multiple lesions in the same organ or involvement of more than one organ (**Table 1**).

The average largest lesion dimension was 4.0±3.6 cm (range 0.6-15.0 cm). The average SUVmax of the most metabolically active lesion at any site was 5.3±3.3 (range 1.2-17.1). In bone lesions, the mean SUVmax was 7.9±5.4 (range 3.5-17.1), in liver lesions the mean SUVmax was 5.1±2.1 (range 2.6-10.5), and in lung lesions the mean SUVmax was 3.0±1.9 (range 1.2-8.5) (**Table 2**). There was no significant difference in the highest SUVmax at any site between patients with an isolated site of disease versus multiple organ involvement (5.5±4.1 vs. 5.0±2.4, *P* = 0.64) or between patients with liver involvement versus those without (5.2±2.3 vs. 5.3±4.5, *P* = 0.93). Patients with bone involvement did trend towards higher overall SUVmax than those without (7.8±5.5 vs. 4.8±2.7, *P* = 0.055), and patients without pulmonary involvement had higher SUVmax at any site than those with lung lesions (6.7±3.9 vs. 4.0±1.2, *P* = 0.012).

Of patients with pulmonary lesions, 9/19 (47%) showed calcification. Of these patients, 7/9 (78%) had nodules with a benign calcification pattern, including 4/9 (44%) with central calcification and 3/9 (33%) with popcorn-like calcification [24]. Only 2/9 (22%) of these patients had nodules with punctate calcifications. Of the patients with pulmonary lesions, 4/19 (21%) had nodules that were either non FDG-avid or < 10 mm and therefore too small for accurate SUV assessment [25-28].

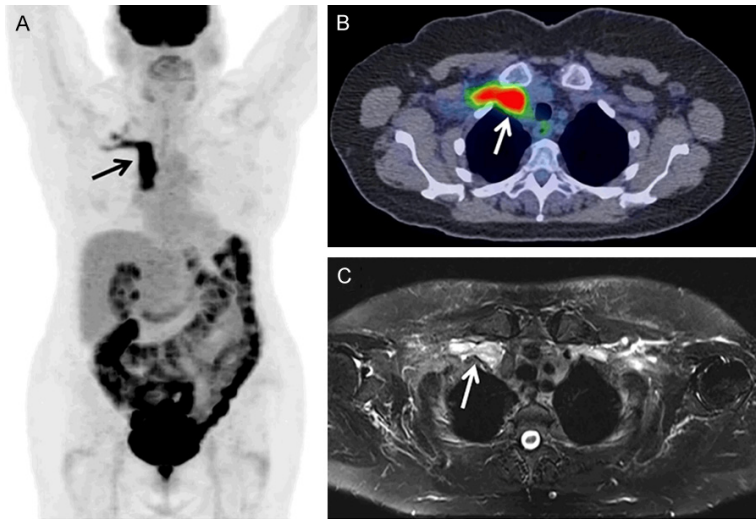
53% (10/19) of patients with pulmonary nodules had imaging follow-up greater than 12 months (range 18 months - 11 years, average 5.2±3.6 years). 70% (7/10) of the patients demonstrated very slow growth of pulmonary lesions, with average volume doubling time of 1154±772 days (range 460-2236 days) and 30% (3/10) had no growth on follow-up images (average time 4.8±5.3 years, range 1.5 to 11 years).

Of patients with hepatic lesions, 19/21 (90%) had at least one FDG avid lesion, 11/21 (52%) demonstrated capsular retraction, and 12/21

**Table 2.** Metabolic characteristics of EHE lesions

Lesion site	Number of patients	SUVmax $\pm$ SD	Range
Liver	21	5.1 $\pm$ 2.1	2.6-10.5
Lung	19	3.0 $\pm$ 1.9	1.2-8.5
Bone	5	7.9 $\pm$ 5.4	3.5-17.1
Most Metabolically Active Site	35	5.3 $\pm$ 3.3	1.2-17.1

SD = standard deviation.


**Figure 1.** 69-year-old female with supraclavicular EHE involving the superior vena cava. FDG PET MIP (A), axial fused PET/CT (B) and axial T2-weighted MRI (C) images demonstrate an intravascular mass with moderate FDG activity (arrows, A, B) and increased T2 signal intensity (arrow, C).

(57%) were found to have additional hepatic lesions on contrast-enhanced CT or MRI that were occult on PET/CT (lesions were too small, had FDG activity equal to background hepatic parenchymal activity, and/or were occult on low-dose non-contrast CT images). Of the patients with bone lesions, 3/5 (60%) were purely lytic and 2/5 (40%) exhibited mixed lytic and sclerotic features.

### Discussion

To our knowledge, this is the largest study examining the FDG PET/CT imaging features of EHE and we found that EHE demonstrates variable, but most commonly moderate FDG activity on PET/CT. In addition, our study confirmed common morphologic features reported by earlier studies, including presence of benign-appearing calcifications in pulmonary lesions and frequent capsular retraction in hepatic lesions.

Although EHE may present in almost any location, it usually affects the soft tissues and visceral organs. As seen in our study, the liver, lung, and bone are the most frequently involved sites. EHE is commonly multifocal with involvement of multiple organs and our results reflected this. 86% (30/35) of our patients presented with multiple lesions, either multiple lesions in the same organ or involvement of more than one organ. While the majority of the patients had pulmonary, hepatic or bone involvement, several patients had less common sites of involvement, including vasculature, mediastinum, retroperitoneum, paracolic soft tissues and gluteal musculature. We also noticed a predilection for vascular involvement in the supraclavicular fossa (**Figure 1**), which was seen in four of our patients. A few prior reports have also described intravascular EHEs arising from large vessels such as the internal jugular

vein [29], inferior vena cava [30], superior vena cava [31], and azygos vein [32].

The pre-existing literature regarding FDG PET/CT in EHE is limited to case reports or small series, and some studies have shown high FDG uptake by EHE [33-35]. For example, Rao reported a patient with multiple EHE lesions involving the pelvic bones and right femur with SUVmax of 18.1 [36]. Our study demonstrated a broad range of FDG activity in EHE lesions, with average SUVmax of the most metabolically active lesion at any site of 5.3 $\pm$ 3.3, and SUVmax range between 1.2 and 17.1. There was no significant difference in the highest SUVmax at any site between patients with an isolated site of disease versus multiple organ involvement. There was also no significant difference in maximal SUVmax between patients with liver disease versus those without. Interestingly, we noted that patients without pulmonary involvement had higher SUVmax



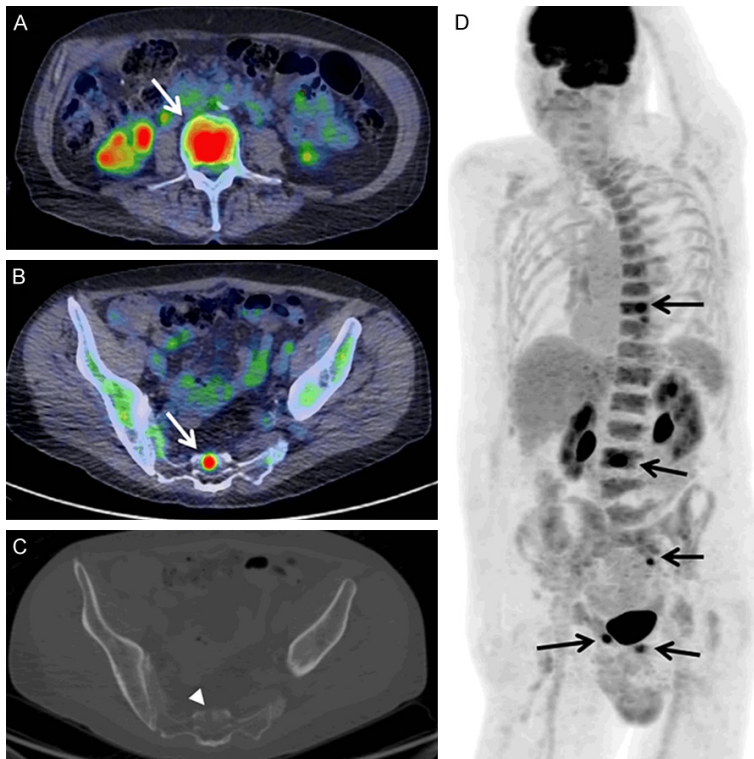


**Figure 2.** 82-year-old male with biopsy-proven osseous EHE. Axial fused PET/CT (A and B), axial CT (C) and FDG PET MIP (D) images demonstrate multiple bone lesions involving the T9 and L3 vertebral bodies, sacrum and bilateral pubic bones with increased FDG activity (arrows A, B and D). The lesions are predominately lytic on CT images (arrowhead, C).

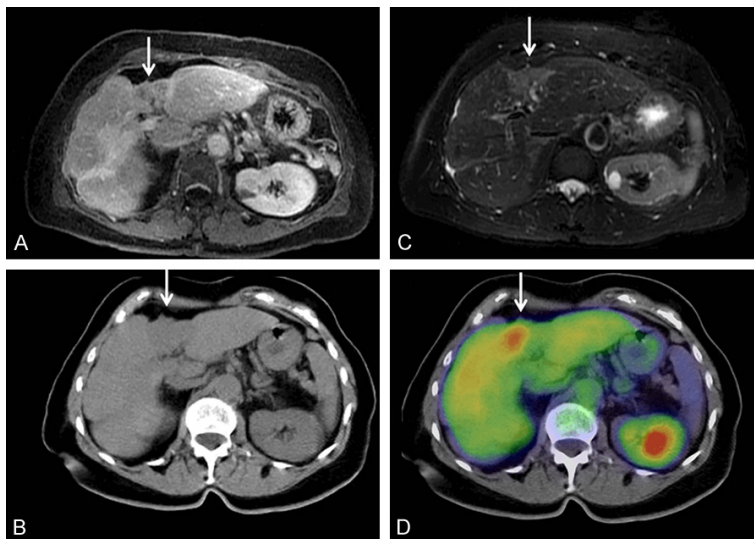


**Figure 3.** 72-year-old female with hepatic EHE. Axial T1-weighted post contrast MRI (A), axial non-contrast CT (B), T2-weighted MRI (C) and fused FDG PET/CT images (D) demonstrate an FDG-avid, enhancing lesion in the right hepatic lobe with capsular retraction (arrows).

higher overall SUVmax in patients with bone lesions (**Figure 2**) compared to those without ( $7.8 \pm 5.5$  vs.  $4.8 \pm 2.7$ ,  $P = 0.055$ ).

Typical CT and MRI features of hepatic EHE have been previously described and include subcapsular location and coalescence of nodules, capsular flattening or retraction, a target-like configuration, and peripheral and delayed central enhancement [21, 22]. Dong and colleagues examined six patients with 60 total hepatic EHE lesions, and found that 40 lesions (67%) demonstrated increased uptake compared to surrounding liver parenchyma [21]. The mean SUVmax of all lesions was  $3.6 \pm 1.1$ , and there was relative low variability among lesions, with SUVmax ranging from 1.7 to 6.6. Ganeshan and colleagues recently reviewed 67 patients with hepatic EHE, 13 of which were evaluated by FDG PET/CT. 8/13 patients had hepatic lesions with FDG uptake above background liver parenchyma. Capsular retraction was reported in 81% (54 of 67 cases) and tumor coalescence in 61% (41 of 67 cases) of the patients [22]. These previous studies examining hepatic EHE were similar to the results in our study. In the 21 patients with hepatic involvement in our cohort, mean SUVmax of the liver lesions was  $5.1 \pm 2.1$  (range 2.6-10.5) and 52% (11/21) of the patients with hepatic lesions demonstrated associated capsular retraction (**Figure 3**). 90% (19/21) of patients with hepatic disease had at least one FDG avid lesion. However, 52% (11/21)

had additional lesions demonstrated on CT or MRI that were not visualized on PET/CT, either

than those with lung lesions ( $6.7 \pm 3.9$  vs.  $4.0 \pm 2.1$ ,  $p = 0.012$ ), and there was a slightly

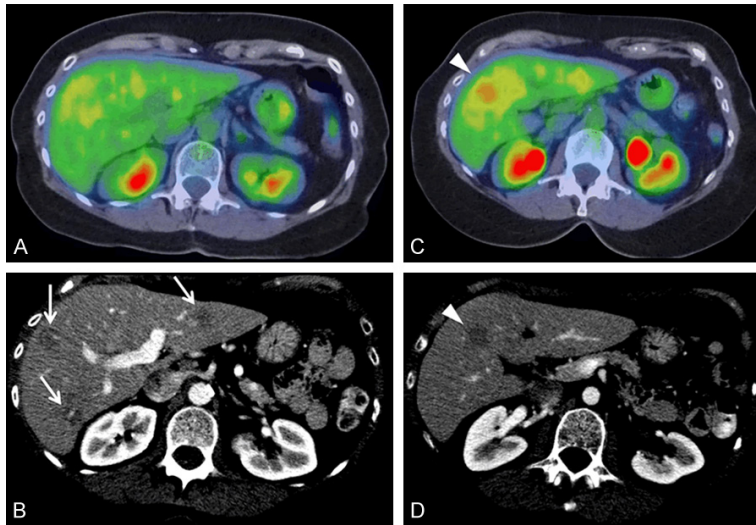


**Figure 4.** 63-year-old female with hepatic EHE. Axial fused PET/CT images (A at portal vein bifurcation and C inferior segments) and axial contrast-enhanced CT (B at portal vein bifurcation and D inferior segments) demonstrate multiple hepatic lesions, some FDG-avid (arrowheads, C and D) and additional lesions seen only on CT (arrows, B).

because of the small size, occult appearance on non-contrast CT, and/or FDG activity equal to background hepatic parenchymal activity (**Figure 4**). This is also similar to previous studies; in the work by Dong and colleagues, 20/60 lesions (33%) had FDG activity similar to background [21], and in the Geneshan cohort, 5/13 patients (38%) had lesions without uptake greater than background hepatic parenchyma. This underscores the importance of utilizing contrast-enhanced CT or MRI in these patients, as PET/CT may miss hepatic lesions.

Pulmonary EHE usually presents as bilateral pulmonary nodules of variable size ranging from 5 to 15 mm, but generally less than 20 mm, as demonstrated in a previous literature review of 93 cases [37]. The nodules can show little or no growth on serial radiographs and are usually found near small and medium sized vessels and bronchi [38]. Volume doubling time (VDT) is defined as the number of days in which a nodule doubles its volume. VDT is a key parameter in lung cancer screening and helps to differentiate between benign and malignant pulmonary nodules. Nodules that remain stable over a period of at least 2 years have a very low probability of malignancy, although 2-year stability does not guarantee a 'benign' nodule because some malignant nodules have a long VDT [39]. Low VDT indicates rapid growth, and a VDT of less than 400 days

has recently been suggested as the best cut-off value to distinguish between 'indolent' and malignant lesions [40, 41]. In our study, 53% (10/19) of patients with pulmonary nodules had imaging follow-up greater than one year (range 18 months - 11 years, average  $5.2 \pm 3.6$  years). 70% (7/10) of the patients demonstrated very slow growth of pulmonary lesions, with average volume doubling time of  $1154 \pm 772$  days (range 460-2236) and 30% had no growth on follow up images after at least 12 months (average  $4.8 \pm 5.3$  years, range 1.5 to 11 years).

In a patient without prior comparison images, the pulmonary nodules of EHE may be mistaken for pulmonary metastatic disease. In patients with serial images, stability or only minimal growth may be mistaken for granulomatous infection or attributed to differences in technique. EHE pulmonary nodules commonly exhibit a benign pattern of calcification, further mimicking sequelae of prior granulomatous diseases, such as histoplasmosis or tuberculosis, pneumoconiosis such as coal workers' pneumoconiosis and silicosis, pulmonary hamartomas, and other benign processes [42]. Our study showed that 47% (9/19) of patients with pulmonary lesions had calcification, 7/9 (77%) of which had a benign pattern, including 4/9 (44%) with central calcification and 3/9 (33%) with popcorn-like calcification. In several cases these nodules mimicked the appearance of pulmonary granulomatous fungal infection (**Figure 5**).

PET/CT data from patients with thoracic EHE has demonstrated variable FDG uptake [43-45]. For example, Woo and colleagues reported PET/CT features of 15 patients with thoracic EHE involvement, and found that the main lesions showed higher uptake than the mediastinal blood pool in 11/15 (73%), and in patients with measurable SUV, a median SUVmax of 5.0, and range of 1.7-14.3. They further observed four different patterns of involvement, including multiple pulmonary nodules,

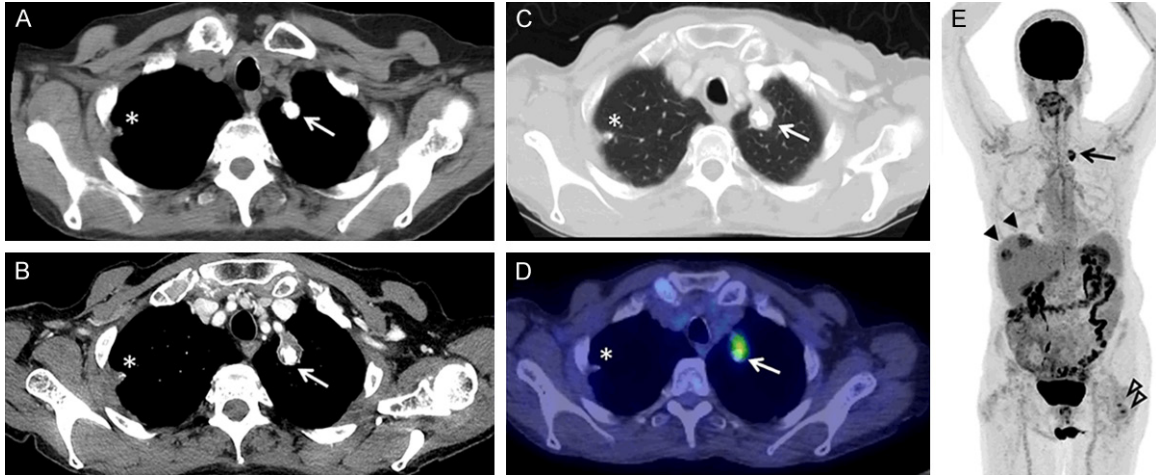


**Figure 5.** 77-year-old female with metastatic EHE. Axial chest CT 2011 (A), axial chest CT 2017 (B and C), axial fused PET/CT (D) and FDG PET MIP (E) images demonstrate calcified bilateral pulmonary nodules (arrows, A-D and asterisks, A, B) with very slowly growth from 2011 to 2017. Note multiple sites of involvement including lung (arrow, E), liver (solid arrowheads, E) and muscle (open arrowheads, E).

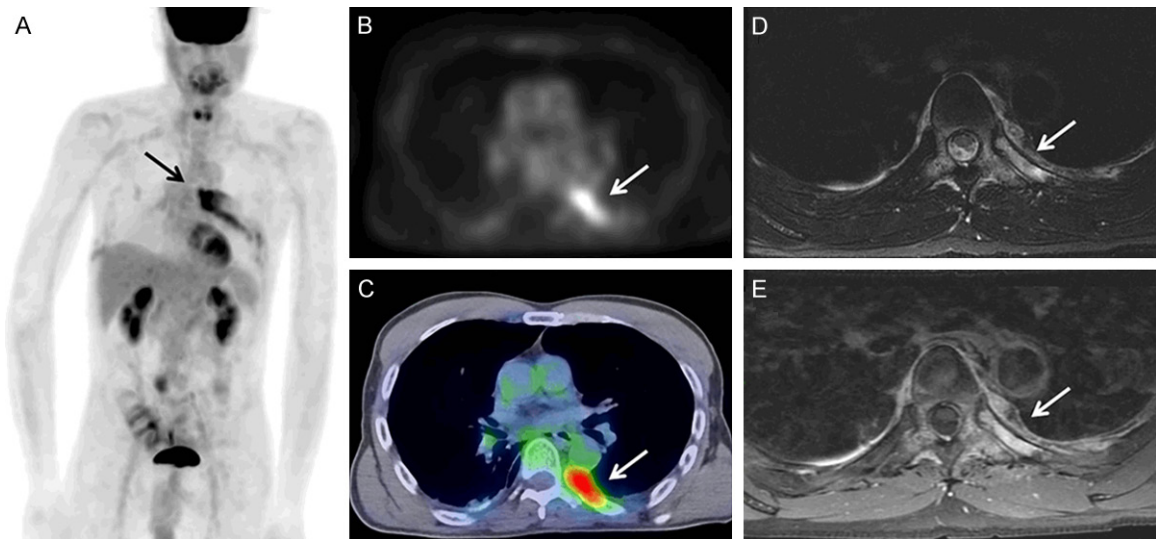


**Figure 6.** 59-year-old male with EHE involving the pleura and ribs. FDG PET MIP (A), axial PET (B), axial fused PET/CT (C), T2-weighted fat-suppressed MRI (D) and axial post-gadolinium T1-weighted fat-suppressed MRI (E) images demonstrate an FDG avid (arrows, A-C), T2 hyperintense (arrow, D), and enhancing (arrow, E) lesion involving the posterior left ribs and adjacent pleural space.

parenchymal tumor with pleural invasion, reticulonodular opacities, and diffuse pleural thickening [46]. In our study, the average SUVmax of the most metabolically active lung lesion was  $3.0 \pm 1.9$  (range 1.2-8.5). However, 4/19 patients with lung lesions (21%) had pulmonary nodules that were either non FDG avid or  $< 10$  mm in size, and thus prone to partial volume effects for SUV calculation. While pulmonary parenchymal involvement is the most common type of thoracic disease, involvement

of the pleura and mediastinum also has been reported. In our study, we found 5/19 patients with pleural involvement (**Figure 6**) and 2/19 with mediastinal involvement. Given that pleural involvement portends a poor prognosis [47, 48], as it may complicate or even prevent surgical resection, it is important to identify and report pleural involvement in EHE patients.

Because of its rarity, EHE has no standard treatment. Surgical resection with clear mar-



gins should be considered for localized disease and may be curative [5]. For hepatic EHE, liver transplant is a management option [33]. The role of adjuvant chemotherapy and radiation therapy is still uncertain, but radiotherapy has been shown to be effective for treatment of bone lesions [7, 8] and several studies have reported therapeutic effect with several drugs, including pazopanib [11], sorafenib [12], and bevacizumab [13]. Suga [49] also demonstrated the utility of FDG PET/CT in assessing response to radiation therapy in the case of hepatic EHE. Given the intrinsic metabolic activity and multi-organ involvement shown in this cohort, PET/CT has clear potential to be useful in these patients, especially for assessing response to both localized and systemic therapies.

Limitations of this study included the small size and retrospective nature. There may have been selection bias in that patients referred for PET/CT may have had more extensive or aggressive disease compared to all EHE patients, many of whom had evaluation by conventional imaging only. In addition, not all patients with  $^{18}\text{F}$ -FDG PET/CT had CT or MRI correlation. Despite these limitations, this is the largest study of its kind and provides evidence that  $^{18}\text{F}$ -FDG PET/CT is a promising modality for EHE evaluation.

## Conclusion

EHE demonstrates variable, but most commonly moderate FDG activity on PET/CT. The most common sites of disease are the liver, lungs, and bones, and most patients present with multiple lesions and more than one organ involved. Given the intrinsic metabolic activity and multi-organ involvement, FDG PET/CT represents an attractive modality for EHE evaluation. However, it may be best used in combination with CT or MRI given that EHE pulmonary or hepatic lesions may be missed by PET/CT.

## Disclosure of conflict of interest

None.

**Address correspondence to:** Dr. Stephen M Broski, Mayo Clinic, Charlton Building North, 1<sup>st</sup> Floor, 200 First Street SW, Rochester, MN 55905, USA. Tel: 507-293-6155; Fax: 507-293-3680; E-mail: Broski.stephen@mayo.edu

## References

- [1] Dail D and Liebow A. Intravascular bronchioalveolar tumor. *Am J Pathol* 1975; 78: A6-A7.
- [2] Weiss SW and Enzinger FM. Epithelioid hemangioendothelioma: a vascular tumor often mistaken for a carcinoma. *Cancer* 1982; 50: 970-981.
- [3] Weiss SW, Ishak KG, Dail DH, Sweet DE and Enzinger FM. Epithelioid hemangioendothelioma and related lesions. *Semin Diagn Pathol* 1986; 3: 259-287.
- [4] Doyle LA. Sarcoma classification: an update based on the 2013 world health organization classification of tumors of soft tissue and bone. *Cancer* 2014; 120: 1763-1774.
- [5] Sardaro A, Bardoscia L, Petruzzelli MF and Portoluri M. Epithelioid hemangioendothelioma: an overview and update on a rare vascular tumor. *Oncol Rev* 2014; 8: 259.
- [6] Wu X, Li B, Zheng C, Hong T and He X. Clinical characteristics of epithelioid hemangioendothelioma: a single-center retrospective study. *Eur J Med Res* 2019; 24: 16.
- [7] Angelini A, Mavrogenis AF, Gambarotti M, Merlino B, Picci P and Ruggieri P. Surgical treatment and results of 62 patients with epithelioid hemangioendothelioma of bone. *J Surg Oncol* 2014; 109: 791-797.
- [8] Yu L, Gu T, Xiu Z, Shi E and Zhao X. Primary pleural epithelioid hemangioendothelioma compressing the myocardium. *J Card Surg* 2013; 28: 266-268.
- [9] Lazarus A, Fuhrer G, Malekiani C, McKay S and Thurber J. Primary pleural epithelioid hemangioendothelioma (EHE)—two cases and review of the literature. *Clin Respir J* 2011; 5: e1-5.
- [10] Kim EA, Lele SM and Lackner RP. Primary pleural epithelioid hemangioendothelioma. *Ann Thorac Surg* 2011; 91: 301-302.
- [11] Semenisty V, Naroditsky I, Keidar Z and Barsela G. Pazopanib for metastatic pulmonary epithelioid hemangioendothelioma—a suitable treatment option: case report and review of anti-angiogenic treatment options. *BMC Cancer* 2015; 15: 402.
- [12] Kobayashi N, Shimamura T, Tokuhisa M, Goto A and Ichikawa Y. Sorafenib monotherapy in a patient with unresectable hepatic epithelioid hemangioendothelioma. *Case Rep Oncol* 2016; 9: 134-137.
- [13] Agulnik M, Yarber JL, Okuno SH, von Mehren M, Jovanovic BD, Brockstein BE, Evens AM and Benjamin RS. An open-label, multicenter, phase II study of bevacizumab for the treatment of angiosarcoma and epithelioid hemangioendotheliomas. *Ann Oncol* 2013; 24: 257-263.



- [14] Kitaichi M, Nagai S, Nishimura K, Itoh H, Asamoto H, Izumi T and Dail DH. Pulmonary epithelioid haemangioendothelioma in 21 patients, including three with partial spontaneous regression. *Eur Respir J* 1998; 12: 89-96.
- [15] Zhou L, Cui MY, Xiong J, Dong Z, Luo Y, Xiao H, Xu L, Huang K, Li ZP and Feng ST. Spectrum of appearances on CT and MRI of hepatic epithelioid hemangioendothelioma. *BMC Gastroenterol* 2015; 15: 69.
- [16] Gan LU, Chang R, Jin H and Yang LI. Typical CT and MRI signs of hepatic epithelioid hemangioendothelioma. *Oncol Lett* 2016; 11: 1699-1706.
- [17] Mao X, Liang Z, Chibhabha F, Ou W, Li N, Xu P and Wang S. Clinico-radiological features and next generation sequencing of pulmonary epithelioid hemangioendothelioma: a case report and review of literature. *Thorac Cancer* 2017; 8: 687-692.
- [18] Mesquita RD, Sousa M, Trinidad C, Pinto E and Badiola IA. New insights about pulmonary epithelioid hemangioendothelioma: review of the literature and two case reports. *Case Rep Radiol* 2017; 2017: 5972940.
- [19] Makis W, Ciarallo A, Nahal A and Derbekyan V. Malignant epithelioid hemangioendothelioma of the lower extremity: staging with F-18 FDG PET/CT. *Clin Nucl Med* 2011; 36: 590-592.
- [20] Parihar AS, Vadi SK, Mittal BR, Singh H, Kumar R and Behera A. (18)F-fluorodeoxyglucose positron emission tomography/computed tomography in childhood metastatic epithelioid hemangioendothelioma of the liver: altering the management plan. *World J Nucl Med* 2019; 18: 183-184.
- [21] Dong A, Dong H, Wang Y, Gong J, Lu J and Zuo C. MRI and FDG PET/CT findings of hepatic epithelioid hemangioendothelioma. *Clin Nucl Med* 2013; 38: e66-73.
- [22] Ganeshan D, Pickhardt PJ, Morani AC, Javadi S, Lubner MG, Elmohr MM, Duran C and Elsayes KM. Hepatic hemangioendothelioma: CT, MR, and FDG-PET-CT in 67 patients-a bi-institutional comprehensive cancer center review. *Eur Radiol* 2020; 30: 2435-2442.
- [23] Ashraf H, Dirksen A, Loft A, Bertelsen AK, Bach KS, Hansen H, Pedersen JH and Mortensen J. Combined use of positron emission tomography and volume doubling time in lung cancer screening with low-dose CT scanning. *Thorax* 2011; 66: 315-319.
- [24] Erasmus JJ, Connolly JE, McAdams HP and Roggli VL. Solitary pulmonary nodules: part I. morphologic evaluation for differentiation of benign and malignant lesions. *Radiographics* 2000; 20: 43-58.
- [25] Zhou Z, Zhan P, Jin J, Liu Y, Li Q, Ma C, Miao Y, Zhu Q, Tian P, Lv T and Song Y. The imaging of small pulmonary nodules. *Transl Lung Cancer Res* 2017; 6: 62-67.
- [26] Imdahl A, Jenkner S, Brink I, Nitzsche E, Stoelben E, Moser E and Hasse J. Validation of FDG positron emission tomography for differentiation of unknown pulmonary lesions. *Eur J Cardiothorac Surg* 2001; 20: 324-329.
- [27] Yilmaz F and Tastekin G. Sensitivity of (18)F-FDG PET in evaluation of solitary pulmonary nodules. *Int J Clin Exp Med* 2015; 8: 45-51.
- [28] Khalaf M, Abdel-Nabi H, Baker J, Shao Y, Lamonica D and Gona J. Relation between nodule size and 18F-FDG-PET SUV for malignant and benign pulmonary nodules. *J Hematol Oncol* 2008; 1: 13.
- [29] Yun JS, Kang SK, Kim SH, Na KJ and Song SY. Epithelioid hemangioendothelioma arising from interanl jugular vein mimicking cervical metastatic lymphadenopathy. *Korean J Thorac Cardiovasc Surg* 2015; 48: 294-297.
- [30] Scordi-Bello IA, Snyder A, Schwartz M and Fallon JT. Intravascular epithelioid hemangioendothelioma of the inferior vena cava: case report of an unusual and unpredictable vascular tumor. *Cardiovasc Pathol* 2009; 18: 243-246.
- [31] Ishibashi H, Takasaki C, Akashi T and Okubo K. Successful excision of epithelioid hemangioendothelioma of the superior vena cava. *Ann Thorac Surg* 2020; 109: e271-e273.
- [32] De Palma A, Pagliarulo V, Ardo N and Loizzi D. Surgical treatment of a rare case of epithelioid hemangioendothelioma of the azygos vein. *Interact Cardiovasc Thorac Surg* 2012; 14: 91-93.
- [33] Lee WW, So Y, Kang SY, So MK, Kim H, Chung HW, Kim WS and Kim SE. F-18 fluorodeoxyglucose positron emission tomography for differential diagnosis and prognosis prediction of vascular tumors. *Oncol Lett* 2017; 14: 665-672.
- [34] Rest CC, Botton E, Robinet G, Conan-Charlet V, Bizais Y and Visvikis D. FDG PET in epithelioid hemangioendothelioma. *Clin Nucl Med* 2004; 29: 789-792.
- [35] Nguyen BD. Epithelioid hemangioendothelioma of the liver with F-18 FDG PET imaging. *Clin Nucl Med* 2004; 29: 828-830.
- [36] Rao M, Chen Y, Huang Z, Zhu Y and Xiao X. FDG PET/CT findings of multifocal epithelioid hemangioendotheliomas of the bones. *Clin Nucl Med* 2015; 40: 821-822.
- [37] Amin RM, Hiroshima K, Kokubo T, Nishikawa M, Narita M, Kuroki M and Nakatani Y. Risk factors and independent predictors of survival in patients with pulmonary epithelioid hemangioendothelioma. Review of the literature and a case report. *Respirology* 2006; 11: 818-825.

- [38] Luburich P, Ayuso MC, Picado C, Serra-Batlles J, Ramirez JF and Sole M. CT of pulmonary epithelioid hemangioendothelioma. *J Comput Assist Tomogr* 1994; 18: 562-565.
- [39] Kanashiki M, Tomizawa T, Yamaguchi I, Kurishima K, Hizawa N, Ishikawa H, Kagohashi K and Satoh H. Volume doubling time of lung cancers detected in a chest radiograph mass screening program: comparison with CT screening. *Oncol Lett* 2012; 4: 513-516.
- [40] Xu DM, van der Zaag-Loonen HJ, Oudkerk M, Wang Y, Vliegenthart R, Scholten ET, Verschakelen J, Prokop M, de Koning HJ and van Klaveren RJ. Smooth or attached solid indeterminate nodules detected at baseline CT screening in the NELSON study: cancer risk during 1 year of follow-up. *Radiology* 2009; 250: 264-272.
- [41] Xu DM, Gietema H, de Koning H, Vernhout R, Nackaerts K, Prokop M, Weenink C, Lammers JW, Groen H, Oudkerk M and van Klaveren R. Nodule management protocol of the NELSON randomised lung cancer screening trial. *Lung Cancer* 2006; 54: 177-184.
- [42] Lee CU, Zreik RT, Boland JM and White ML. Radiologic-pathologic correlation: metastatic pulmonary epithelioid hemangioendothelioma of bone primary. *J Clin Imaging Sci* 2015; 5: 50.
- [43] Albano D, Bosio G, Tironi A and Bertagna F. (18)F-FDG PET/CT in pleural epithelioid hemangioendothelioma. *Asia Ocean J Nucl Med Biol* 2017; 5: 70-74.
- [44] Calabrese C, Gilli M, De Rosa N, Di Crescenzo V, Zeppa P, Vitale C and Vatrella A. Role of FDG-PET scan in staging of pulmonary epithelioid hemangioendothelioma. *Open Med (Wars)* 2016; 11: 158-162.
- [45] Watanabe S, Yano F, Kita T, Soga S, Shinmoto H, Kosuda S, Ozeki Y, Aida S and Sakata I. 18F-FDG-PET/CT as an indicator for resection of pulmonary epithelioid hemangioendothelioma. *Ann Nucl Med* 2008; 22: 521-524.
- [46] Woo JH, Kim TJ, Lee KS, Kim TS and Kim BT. Epithelioid hemangioendothelioma in the thorax: clinicopathologic, CT, PET, and prognostic features. *Medicine (Baltimore)* 2016; 95: e4348.
- [47] Wethasinghe J, Sood J, Walmsley R, Milne D, Jafer A and Gordon-Glassford N. Primary pleural epithelioid hemangioendothelioma mimicking as a posterior mediastinal tumor. *Respirol Case Rep* 2015; 3: 75-77.
- [48] Lee YJ, Chung MJ, Jeong KC, Hahn CH, Hong KP, Kim YJ and Kim YT. Pleural epithelioid hemangioendothelioma. *Yonsei Med J* 2008; 49: 1036-1040.
- [49] Suga K, Kawakami Y, Hiyama A and Hori K. F-18 FDG PET/CT monitoring of radiation therapeutic effect in hepatic epithelioid hemangioendothelioma. *Clin Nucl Med* 2009; 34: 199-202.